PERFORMANCE EVALUATION OF A FASTER-THAN-NYQUIST SYSTEM BASED ON TURBO EQUALIZATION AND LDPC CODES

Albert Abelló (aabellobarberan@eutelsat.com)[1,2], Damien Roque (damien.roque@isae-supaero.fr)[2], Jean-Marie Freixe (jfreixe@eutelsat.com)[1], and Sébastien Mallier (sebastien.mallier@intradef.gouv.fr)[3]

[1]affiliation: Eutelsat SA, Paris, France
[2]affiliation: Institut Supérieur de l'Aéronautique et de l'Espace (ISAE-SUPAERO), Toulouse, France
[3]affiliation: Direction Générale de l'Armement, Rennes, France

ABSTRACT

In the frame of digital video broadcasting by satellite - second generation (DVB-S2), a faster-than-Nyquist (FTN) system based on turbo equalization and low-density parity-check (LDPC) codes is proposed. Truncated *maximum a posteriori* (MAP) and minimum mean square error (MMSE) equalizers provide a reduced-complexity implementation of the FTN system. On the other hand, LDPC codes allow us to demonstrate attractive performance results over an additive white Gaussian noise (AWGN) channel while increasing spectral efficiency beyond the Nyquist rate up to 60 % and keeping a complexity comparable to a current DVB-S2 modem.

1. INTRODUCTION

With an increasing use of wireless communications systems, spectral resources become more and more scarce. In this context, new transmission techniques must offer high spectral efficiency while fulfilling usual constraints in terms of transmitted power and bit-error-probability. In the frame of satellite broadcasting applications, new services such as video on demand combined with an increasing need of quality of service confirm the interest for high density transmission techniques [1].

Traditional systems usually respect the Nyquist criterion in order to avoid inter-symbol interference (ISI): the symbol rate is thus bounded by the bilateral bandwidth of the transmitted signal [2]. Consequently, the only way to improve spectral efficiency relies on an extension of the constellation size. However, given a fixed transmission power, the distance between symbols is decreased such that bit-error-rate (BER) performance necessarily decrease as well.

Another strategy referred to as "faster-than-Nyquist" (FTN) signaling was first introduced by J. Mazo in 1975 [3] in order to improve spectral efficiency without increasing the constellation size. This transmission technique yields unconditionally ISI so that non-linear receivers are required in order to reconstruct the sequence of transmitted symbols. Since a signaling rate increase up to 25% beyond the Nyquist rate keeps a constant minimum distance between symbols, it can be shown that bit-error-probability might remain unchanged at the cost of an extra computational load [4]. Nevertheless, such an algorithmic complexity has prevented the use of FTN techniques for a while.

Recent technological advances combined with iterative equalization and decoding techniques [5, 6] allow FTN systems to be implemented with reasonable complexity. The challenge is therefore to find the best compromise between complexity and spectral efficiency increase. As a consequence, practical FTN systems have been presented and demonstrated attractive performance results [7, 8, 9]. FTN combined with low-density parity-check codes (LDPC) has been proposed in the framework of DVB-S2X [10], but finally postponed in order to avoid significant changes in the architecture of the receivers. More recently, spectral efficiency gains up to 8-20 % have been achieved with the help of linear equalization structures which suggest an affordable implementation cost in user terminals [11, 12].

As an extension of the work aforementioned, we present a faster-than-Nyquist system achieving very attractive performance over the additive white Gaussian noise (AWGN) channel by means of LDPC codes. Our contributions include the comparison between non-linear and linear equalization criteria, based on *maximum a posteriori* (MAP) and minimum mean square error (MMSE), respectively. In the former case, the truncation of the discrete-time FTN channel impulse response is investigated in order to keep an affordable reconstruction complexity.

The article is organized as follows. Part 2 details the input-output relations of the FTN system over an AWGN channel. This includes a linear stage used for pulse shaping and a non-linear stage based on turbo equalization, intended for interference cancellation based on LDPC codes. Two equalization criteria are discussed: truncated MAP and MMSE. Part 3 studies BER system performance through simulations and also discusses its iterative convergence using extrinsic information transfer (EXIT) charts while emphasizing its low additional complexity compared to actual satellite communication systems. Finally, conclusions are presented in part 4.

2. FASTER-THAN-NYQUIST SYSTEM

This part presents the basics of faster-than-Nyquist transmission and the use of turbo equalization techniques. First of all, interference at the output of a linear reveiver is described and modeled as a finite-length discrete equivalent convolutive channel. This channel model will be used by two different equalization techniques presented next. Finally, the turbo equalization principle is introduced as a mean to reach the ISI-free system performance.

2.1. Linear FTN system over an AWGN channel

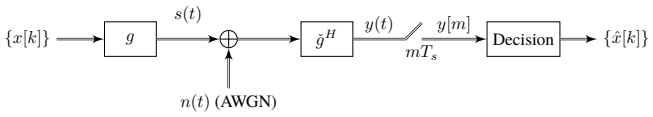

Figure 1: Linear transmission system over an AWGN channel.

We first consider the linear system depicted in figure 1. Let $\{x[k]\}_{k\in\mathbf{Z}} \subset \ell_2(\mathbf{Z})$ be a sequence of independent and identically distributed (IID) symbols to be transmitted, where $\ell_2(\mathbf{Z})$ is the set of square summable sequences. The complex baseband signal at the output of the transmitter is obtained by associating each $x[k]$ to a pulse shape $g(t) \in \mathcal{L}_2(\mathbf{R})$, where $\mathcal{L}_2(\mathbf{R})$ is the set of square integrable signals:

$$s(t) = \sum_{k\in\mathbf{Z}} x[k]\, g(t - kT_s) \quad x[k] \in \mathbf{A}, |\mathbf{A}| = M, t \in \mathbf{R} \quad (1)$$

with T_s the elementary symbol spacing and $\mathbf{A}$ the symbol set of size M (or constellation). Over an AWGN channel, the received signal is denoted $r(t) = s(t) + n(t)$ where $n(t)$ is a circular Gaussian random process with zero-mean and variance σ_n^2.

The received signal $r(t)$ is filtered by $\check{g}^H(t) \in \mathcal{L}_2(\mathbf{R})$, where $\cdot^H$ denotes the conjugate transpose operator. The resulting signal $y(t)$ is then sampled synchronously at times mT_s, $m \in \mathbf{Z}$. If one denotes $h[m] = (g * \check{g}^H)(mT_s)$ the samples from the global transmission-reception filter (*i.e.* discrete-time equivalent channel impulse response) and $w[m] = (n * \check{g}^H)(mT_s)$ the samples of the filtered noise, we have

$$y[m] = \underbrace{x[m]h[0]}_{\text{useful term}} + \underbrace{\sum_{n\in\mathbf{Z}\setminus\{0\}} x[m-n]h[n]}_{\text{interference term}} + \underbrace{w[m]}_{\text{noise term}} \quad (2)$$

where $y[m] = y(mT_s)$. The noise term $w[m]$ is assumed to remain a white process. In practice, this constraint would require the use a whitening filter, not represented here.

Within the linear system aforementioned, we define the system transmission density $\rho = 1/(T_s B)$ where B is the transmitted signal bandwidth (such that $0 < B < +\infty$) at the transmitter side. We identify two cases:

- if $\rho \leq 1$, interference-free transmission can be performed by means of a linear receiver (with Nyquist pulses), in such a case, the system is said orthogonal;
- if $\rho > 1$, inter-symbol-interference unconditionally appears at the output of the linear receiver but if one further assumes that symbols are taken from a finite constellation, they can still be recovered by means of a non-linear post-processing.

The concept of density has only recently been introduced as a definition for FTN systems [13] and it is used throughout this paper. The density criterion is justified by the frame theory [14] in order to determine the existence of ISI-free linear systems.

2.2. Discrete-time equivalent FTN channel

We have seen that since we transmit beyond the Nyquist rate, we must deal with inter-symbol interference. This interference can be seen as if it was produced by a convolutive channel, denoted $\{h[l]\}_{l\in\mathbf{Z}}$ in (2). The knowledge of both system's density and the transmission and reception filters allows us to define such a discrete-time FTN channel.

This characteristic plays a major role in our system's capabilities and complexity. Radio-frequency transmissions being band-limited to reduce interference between consecutive transmission channels, the impulse response is, in theory, not bounded. On the other hand, equalization techniques yield a complexity highly dependent on the discrete-time FTN channel length. To find a compromise between performance and complexity, we analyze the discrete-time FTN channel as a function of system's density and we introduce a truncated channel response. A Nyquist compliant system yields the discrete-time channel presented in figure 2a which corresponds to a memoryless channel impulse response. We present in figure 2b the discrete-time FTN channel obtained when transmitting at a density exceeding the Nyquist rate and using square root-raised-cosine (SRRC) filters.

The strategy of the truncated approach is therefore to consider the most energetic samples of $h[m]$ so that we achieve a significant complexity reduce within the equalizer. Assuming a symmetric impulse response ($h[m] = h[-m]$), a truncation is performed to $L+1$ (odd) coefficients by defining an energy threshold β such that:

$$\sum_{l=-L/2}^{L/2} |h[l]|^2 \leq \beta, \quad \beta \in [0; 1[. \quad (3)$$

We note that $h[m]$ is non-causal and consequently yields a reconstruction delay in practical receivers. In the case mentioned in figure 2b, this delay corresponds to $L/2$ coefficients. In addition, we consider normalized filters $g(t)$ and $\check{g}(t)$ so that $h[0] = (g * \check{g}^H)(0) = 1$.

2.3. MAP and MMSE equalization

We have shown that in faster-than-Nyquist systems, a discrete-time FTN channel can be obtained in order to characterize the ISI produced. In such conditions, the ISI can be mitigated by using well-known equalization techniques. Through this work,

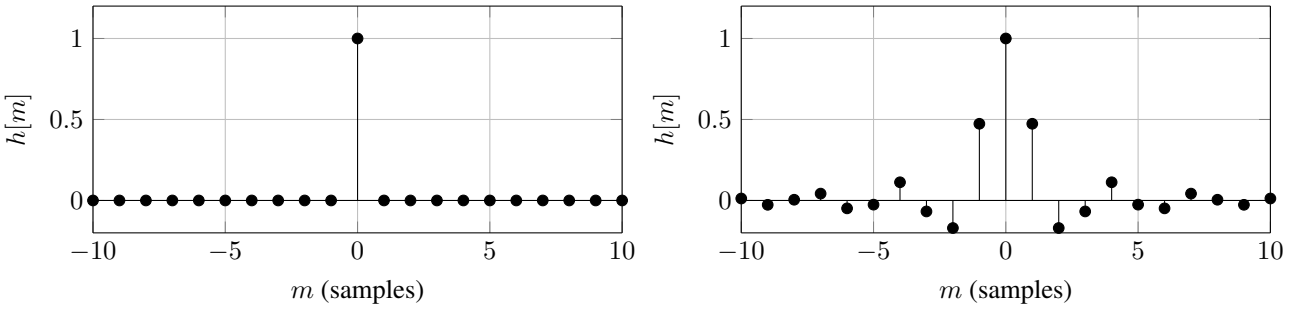

(a) Nyquist rate sampling ($\rho = 0.87$)

(b) Faster-than-Nyquist rate sampling ($\rho = 1.4$)

Figure 2: Discrete-time equivalent channel impulse response with SRRC pulse shapes (roll-off factor $\alpha = 0.15$)

two equalization techniques are considered: *maximum a posteriori* and minimum mean square error. MAP equalization provides us with optimal estimations of the transmitted symbols by maximizing the *a posteriori* probability within a sequence of N transmitted symbols:

$$\hat{x}[k] = \underset{\bar{x}[k]}{\operatorname{argmax}} \ \Pr(\bar{x}[k] = x|\mathbf{y}), \quad x \in \mathbf{A}, k \in \{0, \ldots, N-1\}. \tag{4}$$

with $\bar{x}[k]$ a test symbol, $\mathbf{y} = [y[0], \ldots, y[N-1]]$ a finite sequence of received symbols and $\hat{x}[k]$ the symbol decision at an instant k. The reference algorithm for performing MAP equalization is the so-called BCJR algorithm [15], the strategy of this algorithm being the representation of all possible channel states in a trellis diagram and the recursive computation of symbol likelihoods. In the turbo equalization approach, these estimations depend on *a priori* information provided by the decoder. The limiting factor of this approach is its complexity, since the number of states considered by the MAP equalizer grows exponentially with channel length $L+1$ and with constellation size M. In many applications, this fact makes it impossible to consider MAP equalization techniques. Within an FTN system, the discrete-time channel length will depend on system's density and thus the feasibility of this approach will depend on our spectral efficiency gain and on the alphabet size. For the 21-coefficient channel presented in figure 2b, a MAP equalizer would require computing M^{10} states in order to recursively compute the a posteriori probabilities, with alphabet size M varying from 4 to 32 within DVB-S2 standard. For this reason, the MAP approach is to be considered for small alphabet sizes, in particular for binary phase-shift keying (BPSK) and quadrature phase-shift keying modulations (QPSK).

To deal with this problem, the well-extended MMSE equalization alternative demonstrates attractive performance while keeping a linear dependence on channel length and constellation size. MMSE equalization with *a priori* information is depicted in figure 3.

For each iteration, symbols $\tilde{x}[k],\ k \in \{0, \ldots, N-1\}$ are estimated using *a priori* information from the LDPC decoder. This estimates are then used to make a partial interference cancellation

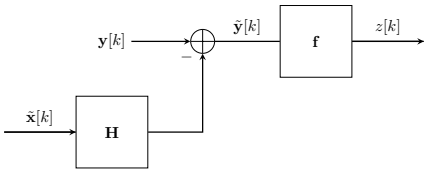

Figure 3: MMSE equalization with *a priori* information.

$$\tilde{\mathbf{y}}[k] = \mathbf{y}[k] - \mathbf{H}\tilde{\mathbf{x}}[k], \quad k \in \{0, \ldots, N-1\} \tag{5}$$

where $\mathbf{y}[k] = [y[k], y[k-1], \ldots, y[k-F+1]]^T$ is a set of channel observations of length F with $\cdot^T$ the transpose operator. $\tilde{\mathbf{x}}[k] = [\tilde{x}[k], \tilde{x}[k-1], \ldots, \tilde{x}[k-F-L]]^T$ is a set of symbol estimates using *a priori* information where $\tilde{x}[k-\delta]$ is set to zero in order not to cancel the useful term, with δ a reconstruction delay. $\mathbf{H}$ is the Toeplitz matrix of size $(F \times F+L)$ formed by the FTN channel impulse response $h[-L/2], \ldots, h[L/2]$. After interference cancellation, linear MMSE filtering is performed:

$$z[k] = \mathbf{f}^T \tilde{\mathbf{y}}[k] \tag{6}$$

where $\mathbf{f} = [f[0], \ldots, f[F-1]]^T$ represents the feedforward filter. Such filter is computed in order to minimize the mean square error between the estimates $z[k]$ and the transmitted symbols $x[k-\delta]$ at an instant $k-\delta$:

$$\mathbf{f} = \underset{\tilde{\mathbf{f}}}{\operatorname{argmin}} \ \mathrm{E}\left\{ \left| \tilde{\mathbf{f}}^T \tilde{\mathbf{y}}[k] - x[k-\delta] \right|^2 \right\} \tag{7}$$

where $\tilde{\mathbf{f}}$ represents the filter variable to be optimized. The choice of the equalization technique will therefore depend on technological considerations, system's complexity having a great impact in terminal's size and consumption. In particular, the discrete-time FTN channel length and the modulation's alphabet will decide whether a MAP implementation is affordable or not.

2.4. System with turbo equalization and LDPC codes

The non-linear system using turbo equalization is depicted in figure 4. Let $\{a[n]\}_{n\in\mathbf{Z}}$ be a sequence IID bits. This sequence is LDPC encoded to produce $\{b[k]\}_{k\in\mathbf{Z}}$. To decorrelate the sequence of coded bits, an interleaver is used, yielding the sequence $\{c[k]\}_{k\in\mathbf{Z}}$. After a bit-to-symbol mapping operation, the sequence $\{x[i]\}_{i\in\mathbf{Z}}$ of transmitted symbols is linearly filtered to output the complex baseband modulated signal $s(t)$ presented in 2.1. Within FTN transmission conditions, the interference term in (2) can be then cancelled by means of a non-linear receiver using the turbo equalization principle [6].

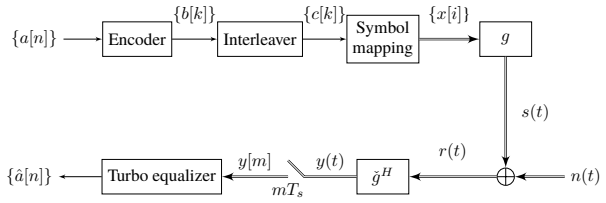

Figure 4: Complete faster-than-Nyquist system with LDPC codes and turbo equalization.

The turbo equalizer principle (fig. 5) consists in an iterative process involving two main blocks: the equalizer performs interference cancellation while the decoder performs an estimation of the sequence of coded bits that will be sent back to the equalizer. The iterative exchange between constituent blocks of the turbo equalizer converges to the orthogonal (ISI-free) system performance. One notes two necessary conditions for system convergence [16]:

1. the sequence between equalizer and decoder must be interleaved and conversely de-interleaved in order to statistically decorrelate the bits;

2. extrinsic information must be exchanged between constituent blocks of the turbo equalizer in order to avoid local convergence. This implies subtracting output and input sequences for each constituent block before sending back the information.

In addition, log-likelihood ratios (LLRs) are used in every iterative step instead of binary values. The LLR of a bit a is given by

$$L(a) = \ln \frac{\Pr(a=1)}{\Pr(a=0)}. \tag{8}$$

By using (8), we define $L(\hat{c}[k]|\mathbf{y})$ the LLRs of equalized interleaved bits $\hat{c}[k]$ knowing $\mathbf{y}$. If the MAP equalizer is used, $L(\hat{c}[k]|\mathbf{y})$ is computed from the a posterior probability in (4). Otherwise, in the case of MMSE equalization, $L(\hat{c}[k]|\mathbf{y})$ results from a soft-input soft-output conversion of (6), as detailed in [6]. Similarly, $L_{ext}(\hat{c}[k]|\mathbf{y})$ and $L_{ext}(\hat{b}[k]|\mathbf{y})$ are the extrinsic LLRs of the estimated bits $\hat{c}[k]$ and $\hat{b}[k]$ knowing $\mathbf{y}$. We denote

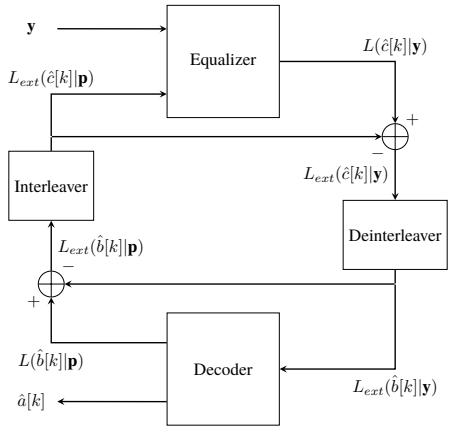

Figure 5: Turbo equalizer block diagram.

$\mathbf{p} = [L_{ext}(\hat{b}[0]|\mathbf{y}), \ldots, L_{ext}(\hat{b}[N-1]|\mathbf{y})]$ the sequence of extrinsic LLRs after de-interleaving, knowing $\mathbf{y}$. Therefore we can define $L(\hat{b}[k]|\mathbf{p})$ the LLRs of the estimated values $\hat{b}[k]$ knowing $\mathbf{p}$, $L_{ext}(\hat{b}[k]|\mathbf{p})$ and $L_{ext}(\hat{c}[k]|\mathbf{p})$ the extrinsic LLRs of the estimated values $\hat{b}[k]$ and $\hat{c}[k]$ knowing $\mathbf{p}$.

The decided sequence $\{\hat{a}[n]\}_{n\in\mathbf{Z}}$ results from performing I iterations within the turbo equalizer. Finally, it is important to note that the non-linear system presented in this section would require, with respect to the DVB-S2 standard system, an additional computational load brought by the equalizer (MAP or MMSE) and by its iterative use along with the channel decoder.

3. SIMULATIONS

In this part, the complete system described previously is simulated in order to evaluate its BER performance as a function of E_b/N_0 where E_b represents the per-uncoded-bit energy and N_0 refers to the noise power spectral density. Extrinsic information transfer (EXIT) charts [17] are also computed. They represent input-output relations of average mutual information between LLRs and input symbols for a given block (equalizer or decoder), denoted $I(L_A; x)$ and $I(L_E; x)$.

The system performs LDPC encoding with code rate $R = 1/2$, a sparse matrix from the DVB-S2 standard [18] and uses a random interleaver. Symbols are IID and follow a BPSK mapping. At the receiver side, iterative MMSE or MAP equalization and LDPC decoding is performed. The turbo equalizer block contains $N = 64800$ symbols. In addition, pulse shapes $g(t)$ and $\breve{g}(t)$ are SRRC with roll-off factor $\alpha = 0.15$. Results show comparable behavior with respect to [12] in terms of convergence for MMSE equalization. Truncated channel MAP performance is compared to performance obtained using MMSE equalization in order to highlight the suitability of the two approaches. Results are compared to the coded orthogonal system performance, performing $\rho = 0.87$ (dashed lines).

BER performance after a given number of turbo iterations is shown in figure 6. For each turbo iteration, the LDPC decoder

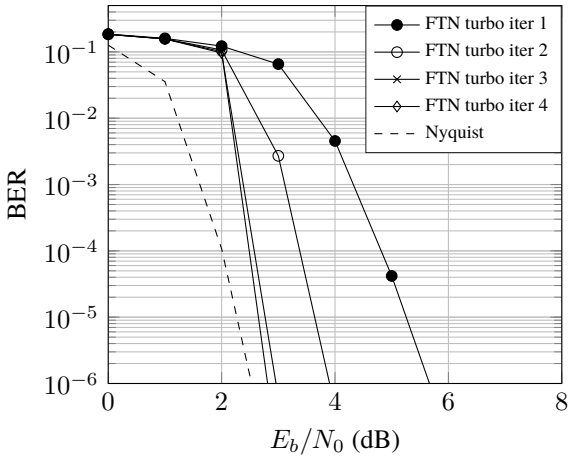

Figure 6: FTN MMSE-LDPC system performance for $\rho = 1.4$ and $\alpha = 0.15$ with 10 LDPC iterations.

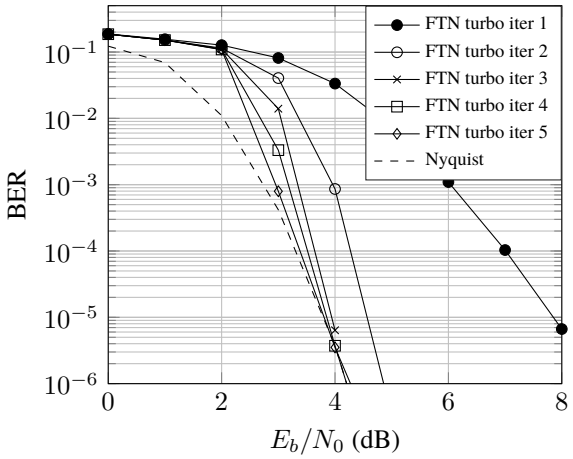

Figure 7: FTN MMSE-LDPC system performance for $\rho = 1.4$ and $\alpha = 0.15$ with 5 LDPC iterations.

performs 10 iterations. Simulations using linear MMSE equalization show that the equalizer becomes the limiting factor when a low LDPC rate is used. One notes the fact that the convergence threshold of 3 dB does not allow to exploit LDPC performance when the latter is configured at 10 iterations. Conversely, a reduction to 5 LDPC iterations (fig. 7) allows us to approach convergence at lower E_b/N_0 values while reducing LDPC complexity. Therefore, this result underlines the need for a joint specification and configuration of the equalizer and the LDPC decoder.

In order to increase system performance while keeping reasonable complexity, results for MAP equalization and LDPC decoding for a 3-coefficient truncated channel (which corresponds to keeping 94 % of channel's energy) are shown in figure 8. Although comparable performance results are obtained for this approach, we are not able to reach convergence for $E_b/N_0 = 4$ dB, the channel model not being representative enough as to the infinite-length channel. In figure 9 are shown system performance for the 5-coefficient truncated channel (97.7 % of channel's energy). We observe that our system outperforms MMSE equalization techniques while keeping reasonable complexity (the recursive algorithm computes 2^5 states). In this case, the system reaches convergence at $E_b/N_0 = 4$ dB after 5 iterations while offering 60 % spectral efficiency increase (from $\rho = 0.87$ to $\rho = 1.4$).

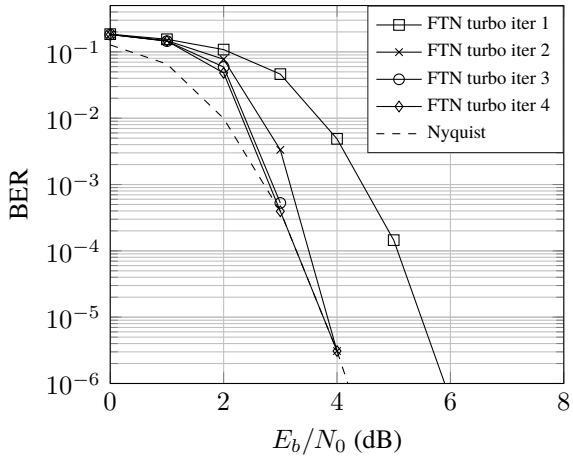

Figure 8: FTN 3-coefficient-truncated MAP-LDPC system performance for $\rho = 1.4$ and $\alpha = 0.15$ with 5 LDPC iterations.

EXIT simulations (fig. 10) allow us to predict system's convergence by representing the exchange of extrinsic information between the two main blocks within the turbo equalizer (equalizer and decoder). We observe that an increase in convergence speed can be obtained when LDPC iterations are increased, two to five iterations being needed to reach the iterative convergence at $E_b/N_0 = 6$ dB. Truncated MAP EXIT simulations confirm that this solution can outperform MMSE realizations while keeping reasonable complexity. The 3-coefficient (94 energy) % truncated channel offers a gain in convergence speed but it shows a suboptimal convergence point in comparison to the MMSE approach: we note an intersection point between 3-coefficient truncaded MAP and MMSE equalization in figure 10. On the other hand, the 5-coefficient (97.7 energy) % truncated MAP equalization would be preferable to the MMSE solution for the system described.

If we exemplify the performance presented in figure 9 with typical DVB-S2 parameters, that is, satellite transponder bandwidth of 36 MHz, QPSK modulation and code rate $R = 1/2$, the given bit rate of 30 Mbit/s could be increased up to 48 Mbit/s while keeping a constant bandwidth and equivalent BER performance for $E_b/N_0 > 4$ dB.

4. CONCLUSION

Through this work, we have presented a faster-than-Nyquist system that could be considered as an evolution of DVB-S2X standard for direct-to-home satellite broadcast. We have shown a 60

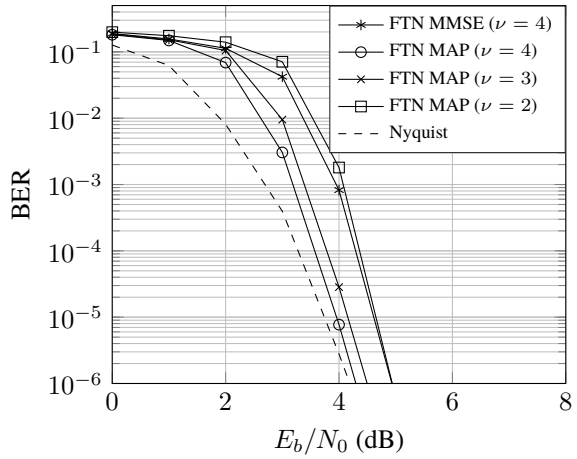

Figure 9: FTN 5-coefficient-truncated MAP-LDPC system performance for $\rho = 1.4$ and $\alpha = 0.15$ with 5 LDPC iterations.

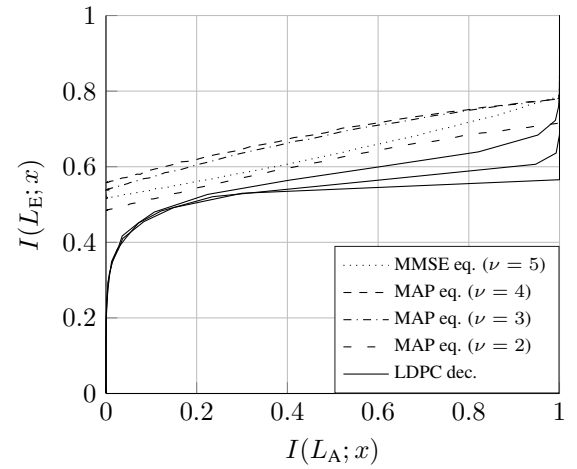

Figure 10: EXIT chart for MAP-LDPC and MMSE-LDPC turbo equalization with $E_b/N_0 = 6$ dB and 2, 3, 4, 5, 10 LDPC iterations.

% spectral efficiency gain with respect to the ISI-free system at the cost of a computational load increase.

The comparison of MMSE and MAP equalization techniques allows us to find a compromise between system performance and complexity. In particular, MAP equalization using truncated discrete-time FTN channels can outperform MMSE solutions by ensuring BER performance convergence at a lower signal-to-noise ratio threshold. However, in virtue of its exponential complexity, the MAP approach is to be considered only for small constellation sizes, in particular for BPSK and QPSK.

Further study on faster-than-Nyquist systems may include the exploration of alternative pulse shapes other than SRRC allowing energy reduction and optimization of the discrete-time FTN channel.

ACKNOWLEDGMENT

This work has been supported by the *Direction Générale de l'Armement* (DGA) under the CIFRE grant 10/2015/DGA.

REFERENCES

[1] R. Emrick, P. Cruz, N. Carvalho, S. Gao, R. Quay, and P. Waltereit, "The sky's the limit: Key technology and market trends in satellite communications," *Microwave Magazine, IEEE*, vol. 15, no. 2, pp. 65–78, March 2014.

[2] H. Nyquist, "Certain topics in telegraph transmission theory," *American Institute of Electrical Engineers, Transactions of the*, vol. 47, no. 2, pp. 617–644, 1928.

[3] E. Mazo, "Faster-than-Nyquist signaling," *Bell. Syst. Tech. Journal*, vol. 54, pp. 1451–1462, Oct. 1975.

[4] G. Forney, "Maximum-likelihood sequence estimation of digital sequences in the presence of intersymbol interference," *Information Theory, IEEE Transactions on*, vol. 18, no. 3, pp. 363–378, 1972.

[5] C. Douillard, M. Jézéquel, C. Berrou, A. Picart, P. Didier, and A. Glavieux, "Iterative correction of intersymbol interference: Turbo-equalization," *European Transactions on Telecommunications*, vol. 6, no. 5, pp. 507–511, 1995.

[6] M. Tüchler and A. Singer, "Turbo equalization: An overview," *Information Theory, IEEE Transactions on*, vol. 57, no. 2, pp. 920–952, 2011.

[7] A. Liveris and C. Georghiades, "Exploiting faster-than-nyquist signaling," *Communications, IEEE Transactions on*, vol. 51, no. 9, pp. 1502 – 1511, sept. 2003.

[8] M. McGuire and M. Sima, "Discrete time faster-than-nyquist signalling," in *Global Telecommunications Conference (GLOBECOM 2010), 2010 IEEE*, dec. 2010, pp. 1 –5.

[9] A. Prlja and J. Anderson, "Reduced-complexity receivers for strongly narrowband intersymbol interference introduced by faster-than-Nyquist signaling," *Communications, IEEE Transactions on*, vol. 60, no. 9, pp. 2591–2601, September 2012.

[10] "ETSI: EN 302 307-2 Digital Video Broadcasting (DVB); Second generation framing structure, channel coding and modulation systems for Broadcasting, Interactive Services, News Gathering and other broadband satellite applications Part II: S2 - Extensions (DVB-S2X)," 2014.

[11] N. Pham, J. Anderson, F. Rusek, J. Freixe, and A. Bonnaud, "Exploring faster-than-Nyquist for satellite direct broadcasting," *AIAA International Communications Satellite Systems Conference*, pp. 16–26, 2013.

[12] G. Maalouli and B. Bannister, "Performance analysis of a MMSE turbo equalizer with LDPC in a FTN channel with application to digital video broadcast," in *Signals, Systems and Computers, 2014 48th Asilomar Conference on*, Nov 2014, pp. 1871–1875.

[13] C. Siclet, D. Roque, H. Shu, and P. Siohan, "On the study of faster-than-Nyquist multicarrier signaling based on frame theory," in *Wireless Communications Systems (ISWCS), 2014 11th International Symposium on*, Aug 2014, pp. 251–255.

[14] O. Christensen, *Frames and bases: An introductory course*. Birkhauser, 2008.

[15] L. Bahl, J. Cocke, F. Jelinek, and J. Raviv, "Optimal decoding of linear codes for minimizing symbol error rate (corresp.)," *IEEE Trans. Inf. Theor.*, vol. 20, no. 2, pp. 284–287, Sep. 2006. [Online]. Available: http://dx.doi.org/10.1109/TIT.1974.1055186

[16] R. Koetter, A. Singer, and M. Tuchler, "Turbo equalization," *Signal Processing Magazine, IEEE*, vol. 21, no. 1, pp. 67–80, Jan 2004.

[17] J. Hagenauer, "The EXIT chart - introduction to extrinsic information transfer in iterative processing," in *Proc. 12th Europ. Signal Proc. Conf (EUSIPCO*, 2004, pp. 1541–1548.

[18] "ETSI: EN 302 307 Digital Video Broadcasting (DVB); Second generation framing structure, channel coding and modulation systems for Broadcasting, Interactive services, News Gathering and other broadband satellite applications (DVB-S2)," 2009.